Joint Special Interest Group meeting between euspen and ASPE
Advancing Precision in Additive Manufacturing
TU Berlin, Germany, October 2025
www.euspen.eu

Opening up new realms of precision, accuracy and throughput via process-optimized two-photon polymerization

J. Rodriguez[1,2], Anna-Maria Fuchsberger[1], G. Winkler[1]

[1]*UpNano GmbH, Austria*
[2]*University of Applied Sciences Upper Austria, Austria*

georg.winkler@upnano.com

Abstract
In photopolymer-based micro-additive manufacturing, the application areas of two-photon polymerization (2PP) and projection micro-stereolithography (PµSL) overlap in terms of the overall achievable part sizes, in the range from a few hundred micrometers to centimeters. Within that range, 2PP is well known for enabling manufacturing with sub-micrometer precision, while PµSL emphasizes throughput at lower resolution. However, the fundamentally different printing mechanisms make it difficult to compare performance based on primary machine parameters. This underlines the need for thorough statistical evaluation of representative prints to accurately assess process capabilities and avoid misleading conclusions about performance trade-offs. Based on a reliable automated analysis of part dimensions, we take a detailed look at both repeatability (intrinsic printer precision) as well as a multitude of effects (often much larger than the bounds on precision) that affect dimensional accuracy. Final data, including throughput, is compared for identical part geometry between 2PP and PµSL. The 2PP system was deliberately set up in a low-resolution/high-throughput configuration, using a 5x objective and *Adaptive Resolution* technology [1] to stretch the voxel size laterally. Compared to a PµSL machine with a nominal resolution of 10 µm, the results show a 12-fold higher precision (12-fold higher capability index) for the 2PP prints at comparable throughput. When compared to a PµSL machine with a nominal resolution of 2 µm, the results show a 5 times higher precision and 11 times higher throughput for 2PP prints. These findings suggest that recent technological advances in 2PP allow to simultaneously provide much higher precision and throughput than PµSL, and even closely match the throughput of PµSL systems that have an order of magnitude lower precision.

Ultra-precision, Accuracy, Laser, Polymer

1. Introduction

While PµSL offers potential throughput advantages through layer-wise parallelization, the actual precision of printed parts typically falls significantly short of the advertised nominal resolution, due to limitations inherent to the single-photon process [2]. In contrast, 2PP enables manufacturing with sub-micrometer precision owing to the strongly localized material interaction in the focus of a fs-laser [3].

Technological advances in 2PP, including Adaptive Resolution, which dynamically adjusts the voxel size for efficient multi-scale printing, enable a significant increase in throughput towards batch production [1]. Moreover, in vat-based 2PP the voxel is kept at a constant height above the bottom of the vat, creating a consistent liquid interface below the part [4]. In contrast to PµSL, there is no need to delaminate the part from the bottom of the vat after each layer, which can damage delicate parts and adds a time delay of typically 4–5 s per layer [5].

In both cases, the question of how the printing process can be optimized for maximum absolute dimensional accuracy in practical parts is often overlooked.

To enable a direct comparison of these two 3D printing technologies, we analyzed 2PP prints of the structure shown in Figure 1a, which is discussed in a similar manner by a whitepaper about PµSL [6]. Based on a reliable automated analysis of part dimensions, we take a detailed look at both part repeatability (intrinsic printer precision) as well as a multitude of effects (often much larger than the bounds on precision) that affect dimensional accuracy. The latter include mechanical influences such as beam steering and thermal drifts, chemical effects such as global shrinkage, boundary erosion and material batch variations, as well as anisotropic exposure, or the optimization of slicer algorithms, among others. We predictively model these effects to optimize dimensional accuracy without requiring part-specific iterative finetuning. The corresponding tests have been conducted using more simplified geometries shown in Figure 1b.

2. Methodology

2.1. 2PP 3D printing

To fabricate the test geometries, the high-resolution 2PP 3D printing system NanoOne 1000 (UpNano GmbH) was used, in which a fs-laser (90 fs pulse length, 80 MHz repetition rate, 780 nm central wavelength) is scanned via a galvo mirror and focused through a microscope objective into a 2PP resin (UpPhoto, UpNano GmbH) reservoir to cure the target structure line-by-line, layer-by-layer. UpNano's *Adaptive Resolution* technology (allowing for dynamic control of the lateral voxel extent) [1] in combination with a choice of objective magnification spanning more than an order of magnitude, allows to serve vastly different printing scenarios. In the present case, the lowest resolution standard objective of the NanoOne system (Fluar 5x/0.25, Zeiss) and *coarse scanning mode* (line spacing of 8 µm, layer spacing of 10 µm) were selected to print parts in the millimeter range (Figure 1) at the highest possible throughput rate while maintaining precision and accuracy in the µm range. By using 2PP vat print mode (in which the fixed-focus objective and resin reservoir are moving in tandem), the part

dimensions are only limited by the motion range of the XYZ-stage that moves the substrate to stitch multiple field-of-views (FOVs) of the objective [4].

Finished parts were developed in two subsequent baths with propylene glycol methyl ether acetate (PGMEA) for 5 min each, followed by a quick dip in isopropyl alcohol (IPA).

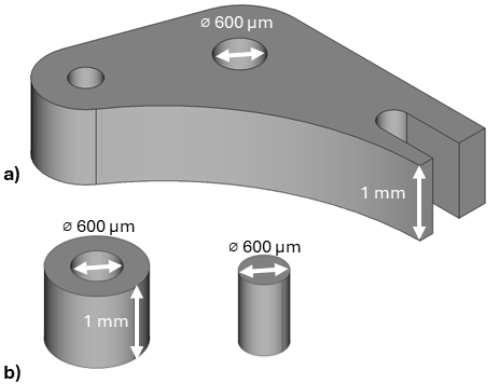

Figure 1. Test geometries printed using 2PP and evaluated in this study: a) Reference part for direct comparison with equivalent results for PµSL [6], b) Simplified geometries to study various influences on dimensional accuracy.

2.2. Automated statistical analysis of circular features

To optimize the printing parameters, each change requires a statistical analysis of a larger batch of nominally identical parts (typically at least 25). To speed up handling, an automated optical measurement process was developed. Common optical metrology lab-devices that provide 3D data (such as laser scanning microscopes or white light interferometers) are notoriously bad at resolving marginally rounded corners - which naturally occur for resin printing - with the required precision.

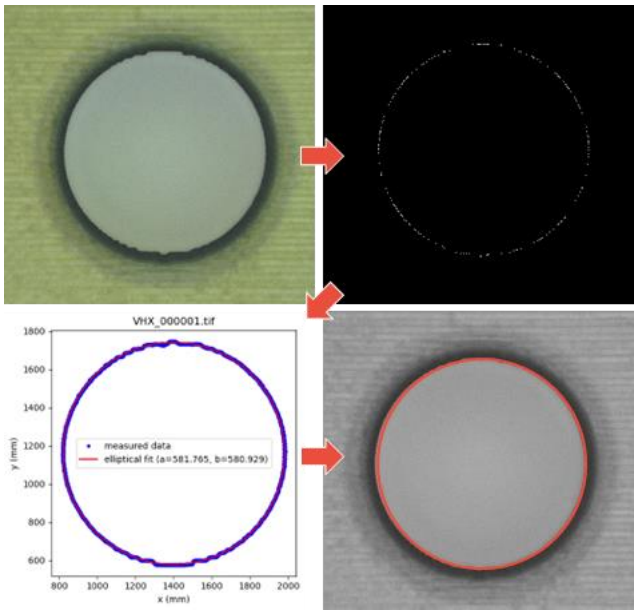

Figure 2. Evaluation steps of the automated statistical analysis of circular features: originally captured 2D high-contrast image; edge detection and rejection of outliers; least-squares fitting; overlay of final result.

Instead, a digital optical microscope (Keyence VHX-7000) was used to record 2D images with high contrast coaxial illumination, followed by automated fitting of an elliptic contour to the through-holes considered for analysis. The algorithm involves a sequence of edge detection (Canny edge detector [7]) followed by a coarse search for circular features (generalized Hugh Transform [8]) and precise least-squares fitting of the elliptical contour to the edge points preselected in the previous step (see Figure 2 for a typical sequence).

This method has been cross-checked by comparison to standard-traceable mechanical profilometer measurements using a micro-probe (ScopeCheck® with Fiber Probe, Werth).

3. Results and discussion

3.1. Comparison of process capability (precision and accuracy)

Already with a sample size of 25, the diameter measurements for 2PP prints of the reference structure (Figure 1a) visibly follow a normal distribution according to Figure 3, which further confirms the measurement routine described in section 2.2. The excellent precision (standard deviation σ of only 0.5 µm) is intrinsic to the highly localized 2PP polymerization process and attainable without further optimization. Accuracy on a similar level is displayed (mean µ of 600.6 µm is only deviating from the nominal Diameter E[x] by 0.6 µm), by following the prescriptions of section 3.2.

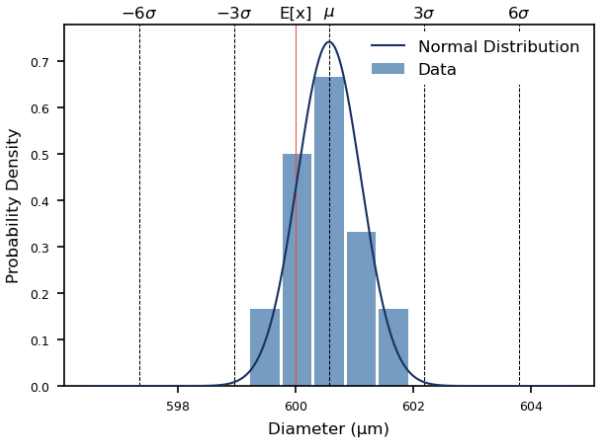

Figure 3. Results for the through-hole with a nominal diameter of 600 µm of the 2PP 3D printed reference geometry shown in Figure 1a. (Sample size N = 25, standard deviation σ = 0.5 µm, mean μ = 600.6 µm).

Two common process capability indices can be used to gauge compatibility of a production process with given lower and upper specification limits (LSL, USL) in terms of precision (C_p) or precision and accuracy (C_pk):

$$C_\mathrm{p} = \frac{USL-LSL}{6\sigma}, \qquad (1)$$

$$C_\mathrm{pk} = \frac{min\,(\mu-LSL, USL-\mu)}{3\sigma} \qquad (2)$$

A C_p value of 2 (meaning a $\mu \pm 6\sigma$ region falling within the specified bounds) is considered a high-quality "Six Sigma" quality process [9]. With C_p and C_pk values of about 16 for the specification limits stated in [6], the "Six Sigma" criterion is easily achieved, surpassing the PµSL results by a factor of more than 12 (see Table 1 for a side-by-side comparison of numerical results). The stated specification limits are used primarily for the sake of direct comparison, as the 2PP results would typically be a match for a much more tightly bounded process.

Table 1. Comparison of process capability between 2PP (NanoOne, UpNano) and PµSL [6].

	μ (µm)	σ (µm)	LSL (µm)	USL (µm)	C_p	C_{pk}
2PP (NanoOne)	600.6	0.5	575	652	16.6	16.3
PµSL (10 µm)[6]	602.7	6.5	575	652	1.3	1.1

These differences between 2PP and PµSL can directly be ascribed to unique properties of the vastly different printing schemes (see comparison in Figure 4). PµSL uses a 2D array of fixed-size pixels (where the effective resolution achieved is heavily limited by bleeding effects associated with non-spatially-selective single-photon excitation). In contrast, in 2PP very well-defined voxels (determined by the 2PP threshold) are scanned and cured sequentially at high speed. The process is highly adaptable to specific resolution requirements (via change of print mode and/or printing objective) [4].

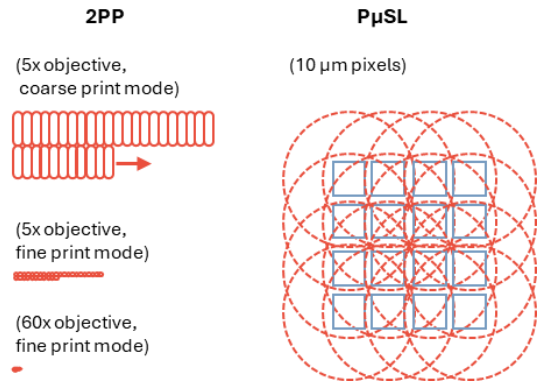

Figure 4. Phenomenological visual comparison of 2PP vs. PµSL printer resolution. 2PP utilizes voxel scanning and offers a wide range of objectives to cover a very broad resolution range. Adaptive Resolution additionally allows to dynamically stretch the lateral voxel size (coarse mode). PµSL uses an array of fixed-size pixels. Dashed lines indicate pixel bleeding (by about a factor of 5 [6]) of the single-photon PµSL process.

3.2. Improving Accuracy

While precision (a.k.a. reproducibility, statistical uncertainty) is intrinsic to the performance of the machine hardware, it is usually possible to optimize dimensional accuracy within the bounds of precision. This can be achieved by means of proper calibration, parameter tuning, and suitable adaptation of the target design geometry.

Improvements are obtainable either via brute force iterative correction [10] (by determining deviations from target via a test print, then adding them with negative sign as corrections to the next print until tolerances are met), or by leveraging more systematic understanding of (dominantly polymerization) effects to predict the necessary corrections directly.

Here, we list several contributing effects and possible countermeasures, with Figure 5 serving as a source of supporting datasets (in the following referenced by number), that have been extracted from 2PP printed circular geometries (Figure 1 b).

- Precise calibration of the galvo scanner is required at a targeted sub-micron level. The NanoOne printer offers an automated procedure for this. Any remaining deviations of suboptimal calibration can be visualized by printing single circular lines directly onto a substrate where they are fixed in place and immune to shrinkage effects (Figure 5, dataset 1).
- Global uniform shrinkage of the polymer caused by volumetric loss during crosslinking can be observed by comparing the previous test to individual circles placed on a printed base (dataset 2) (amounting to about 1% in the present case). The effect can be counteracted by appropriate scaling of the structure prior to printing.
- Surface erosion, by contrast, refers to localized material loss at feature boundaries, typically manifesting as increased inner diameters (dataset 3) and reduced outer diameters (dataset 5), offset both by roughly equal and constant amounts (here approximately ± 5 µm). This likely results from reduced laser exposure dose at surfaces resulting in localized underpolymerization and correspondingly increased volumetric loss during

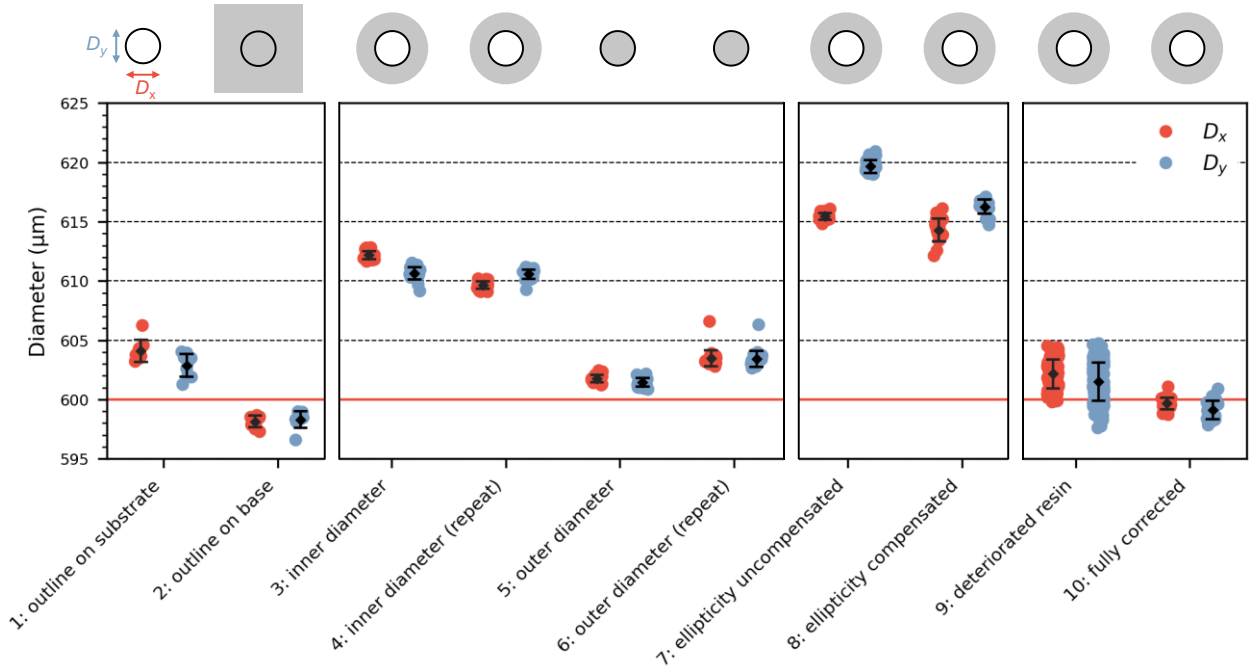

Figure 5. Datasets illustrating various influences on accuracy. For each dataset, the diameter of nominally 600 µm for the innermost feature (marked in black) is plotted in x- and y- direction to simultaneously monitor elliptical deformations.

development [11]. Increasing infill power, as well as reducing coarse line width and coarse line spacing can counteract the inhomogeneities slightly, but a counter-correction of the target geometry (currently on CAD level) is fundamentally needed.

- Temperature fluctuations in the machine environment or varying timespans used for thermalization of substrates and/or mounting components before printing, can lead to small changes between repeated prints (compare datasets 4 and 6)
- Anisotropic distortions of surfaces can occur due to elongation and anisotropic behaviour of the voxel [11], [12] in coarse mode (holes are noticeably elliptical in dataset 7). A "coarse width compensation" parameter in the NanoOne control software (Think3D version >2.5, UpNano) allows for direct correction (applied in dataset 8), often reducing residual ellipticity of the 600 µm holes to below 1 µm.
- Resin ageing (possibly related to prolonged exposure to air [13]), can cause a noticeable decrease in precision (dataset 9). Minimal dimensional variations (±1–2 µm) were routinely observed between different resin batches, generally suggesting very consistent material performance. For utmost precision, it is recommended to finetune the printing process using the same final production batch.
- The "*Voxel Mode*" slicer strategy should generally be chosen to best represent the target geometry [1].

3.3. Comparison of throughput vs. precision

The throughput data summarized in Figure 6 was extracted from benchmark prints on a 2PP printing system (NanoOne, UpNano) and a PµSL machine (microArch S240, BMF) with 10 µm resolution. It is assumed that the print throughput of a 2 µm PµSL machine scales with pixel (or FOV) size. Precision is plotted as inverse standard deviation (scaling linearly with C_p and C_{pk} values for given process-dependent specification limits) with data taken from Table 1 and additional published data comparing different PµSL systems [6]. A typical 50% filling ratio of the build volume is assumed for comparability (to first approximation, 2PP throughput scales with part volume, while PµSL throughput scales with enclosed build volume). Setup times are not considered in that comparison, but are negligible for NanoOne 2PP systems, in particular due to live slicing and fast automatic substrate alignment.

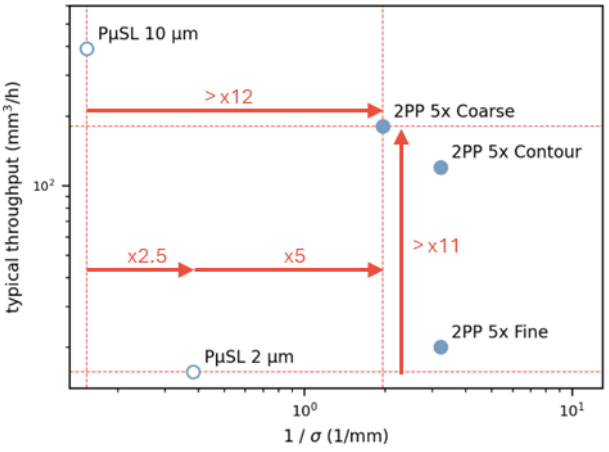

Figure 6. Comparison of throughput vs. precision of PµSL systems with different nominal resolution [6] and NanoOne 1000 (UpNano) equipped with a 5x objective employing different print modes. Precision is indicated by inverse standard deviation. Throughput refers to active print time (without setup time) and actual part volume.

According to the data, 2PP yields 12-fold higher precision at comparable throughput (PµSL 10 µm), or 5-fold higher precision and 11-fold larger throughput compared to the highest-resolution PµSL system (2 µm).

4. Conclusion

Our findings demonstrate that recent technological advances have positioned 2PP as the prime choice for high-precision additive manufacturing of polymer parts requiring tolerances (specification limits) of several tens of micrometers or below. With next-generation systems heavily employing parallelization schemes for laser beam writing, this proposition will be strengthened even further.

References

[1] Lunzer, M., Butterfield, A. N., Karpos, K., Schlepütz, C. M., Kirian, R., and Heymann, M. 2023 Adaptive resolution two-photon 3D printing with X-ray tomographic resolution optimization of ultracompact 3D microfluidics. [Online]. Available: https://www.euspen.eu/knowledge-base/AM23112.pdf

[2] Ge, Q. *et al.* Jun. 2020 Projection micro stereolithography based 3D printing and its applications *Int. J. Extrem. Manuf.* vol. 2, no. 2 p. 022004,

[3] Skliutas, E. *et al.* Mar. 2025 Multiphoton 3D lithography *Nat Rev Methods Primers* vol. 5, no. 1 p. 15,

[4] Koch, T. *et al.* Aug. 2024 Approaching Standardization: Mechanical Material Testing of Macroscopic Two-Photon Polymerized Specimens *Advanced Materials* vol. 36, no. 34 p. 2308497,

[5] Lin, Y.-S. and Yang, C.-J. 2019 Spring Assisting Mechanism for Enhancing the Separation Performance of Digital Light Process 3D Printers *IEEE Access* vol. 7 pp. 71718–71729,

[6] 3D Printing Tolerances and Why They're Important. Accessed: Jun. 01, 2025. [Online]. Available: https://bmf3d.com/blog/3d-printing-tolerances-and-why-theyre-important/

[7] Canny, J. Nov. 1986 A Computational Approach to Edge Detection *IEEE Trans. Pattern Anal. Mach. Intell.* vol. PAMI-8, no. 6 pp. 679–698,

[8] Ballard, D. H. Jan. 1981 Generalizing the Hough transform to detect arbitrary shapes *Pattern Recognition* vol. 13, no. 2 pp. 111–122,

[9] Montgomery, D. C. Introduction to Statistical Quality Control.

[10] Ristok, S., Thiele, S., Toulouse, A., Herkommer, A. M., and Giessen, H. Oct. 2020 Stitching-free 3D printing of millimeter-sized highly transparent spherical and aspherical optical components *Opt. Mater. Express* vol. 10, no. 10 p. 2370,

[11] Plant, R. Optimising laser stereolithography for constructing electronic packages onto novel substrates. [Online]. Available: https://eprints.nottingham.ac.uk/77441/

[12] Wang, H. *et al.* Sep. 2023 Two-Photon Polymerization Lithography for Optics and Photonics: Fundamentals, Materials, Technologies, and Applications *Adv Funct Materials* vol. 33, no. 39 p. 2214211,

[13] Drobecq, I., Bigot, C., Soppera, O., Malaquin, L., and Venzac, B. Apr. 2025 Optimizing dimensional accuracy in two-photon polymerization: Influence of energy dose and proximity effects on sub-micrometric fiber structures *Additive Manufacturing* vol. 103 p. 104735,